

## Low field intergranular tunneling effect in CrO<sub>2</sub> nanoparticles and characterization of the barriers

Jianbiao Dai and Jinke Tang

Citation: *Journal of Applied Physics* **89**, 6763 (2001); doi: 10.1063/1.1362641

View online: <http://dx.doi.org/10.1063/1.1362641>

View Table of Contents: <http://scitation.aip.org/content/aip/journal/jap/89/11?ver=pdfcov>

Published by the [AIP Publishing](#)

---

### Articles you may be interested in

[Magnetic cluster glass behavior and grain boundary effect in Nd<sub>0.7</sub>Ba<sub>0.3</sub>MnO<sub>3</sub> nanoparticles](#)  
J. Appl. Phys. **104**, 103915 (2008); 10.1063/1.3021463

[A large low-field tunneling magnetoresistance of CrO<sub>2</sub> / \( CrO<sub>2</sub>/Cr<sub>2</sub>O<sub>3</sub> \) powder compact with two coercivities](#)  
J. Appl. Phys. **97**, 073907 (2005); 10.1063/1.1868080

[Magnetic inhomogeneity and valence state in Sr<sub>2</sub>CrWO<sub>6</sub> double perovskite](#)  
J. Appl. Phys. **93**, 471 (2003); 10.1063/1.1524710

[Interface characterization and thermal stability of Co/Al–O/CoFe spin-dependent tunnel junctions](#)  
J. Appl. Phys. **91**, 7475 (2002); 10.1063/1.1452228

[Characterization of the natural barriers of intergranular tunnel junctions: Cr<sub>2</sub>O<sub>3</sub> surface layers on CrO<sub>2</sub> nanoparticles](#)  
Appl. Phys. Lett. **77**, 2840 (2000); 10.1063/1.1320845

---

The advertisement features a blue background with a film strip on the left side. The text is centered and reads: 'Not all AFMs are created equal' in orange, 'Asylum Research Cypher™ AFMs' in white, and 'There's no other AFM like Cypher' in orange. At the bottom, the website 'www.AsylumResearch.com/NoOtherAFMLikeIt' is listed in white, and the Oxford Instruments logo is in the bottom right corner with the tagline 'The Business of Science®'.

**Not all AFMs are created equal**  
**Asylum Research Cypher™ AFMs**  
**There's no other AFM like Cypher**

[www.AsylumResearch.com/NoOtherAFMLikeIt](http://www.AsylumResearch.com/NoOtherAFMLikeIt)

**OXFORD**  
INSTRUMENTS  
*The Business of Science®*

# Low field intergranular tunneling effect in CrO<sub>2</sub> nanoparticles and characterization of the barriers

Jianbiao Dai and Jinke Tang<sup>a)</sup>

*Department of Physics, University of New Orleans, New Orleans, Louisiana 70148*

The magnetoresistance (MR) and microstructures of half-metallic CrO<sub>2</sub> nanoparticle systems were studied. Using field alignment, the needle-shaped CrO<sub>2</sub> single domain particles were aligned in the same orientation. The MR of this structure showed a magnetic junction-like behavior with two well-separated peaks in the MR at coercivity fields and the MR of the aligned CrO<sub>2</sub> particles reached >41% at a relatively low field of about 1000 Oe. The magnetotransport mechanism was analyzed in terms of spin dependent tunneling between CrO<sub>2</sub> nanoparticles. Using transmission electron microscopy, x-ray diffraction, and x-ray photoelectron spectroscopy techniques, the intergranular tunneling barrier was characterized to be a very thin Cr<sub>2</sub>O<sub>3</sub> interface layer between the CrO<sub>2</sub> particles. Temperature dependence of MR and conductivity in cold-pressed CrO<sub>2</sub> nanopowders were studied. The MR significantly decreased with increasing temperature and the spin independent hopping conduction is suggested to be responsible for the suppression of MR at high temperature.

© 2001 American Institute of Physics.

[DOI: 10.1063/1.1362641]

## I. INTRODUCTION

Chromium dioxide (CrO<sub>2</sub>) has been predicted to be a half-metallic material by Schwarz using band structure calculation in 1986.<sup>1</sup> The high spin polarization close to 100% of CrO<sub>2</sub> has been demonstrated by different experiments, including photoemission experiment,<sup>2</sup> superconducting point contact experiment,<sup>3</sup> and vacuum tunneling measurement.<sup>4</sup> The nearly perfect spin polarization of CrO<sub>2</sub> suggests that it would be ideal for applications in a ferromagnetic tunneling junction device,<sup>5</sup> where a large magnetoresistance (MR) ratio is expected. It has been reported by Huang *et al.*<sup>6</sup> and Suzuki *et al.*<sup>7</sup> that CrO<sub>2</sub> thin films can have negative MR of about 13%–25% at low temperature. In 1998, Manoharan *et al.*<sup>8</sup> and Coey *et al.*<sup>9</sup> studied the cold-pressed CrO<sub>2</sub> powder samples and found that the MR of the pressed compacts can reach as high as 30%–50% at a magnetic field of about several tesla. The conduction mechanism of these CrO<sub>2</sub> powder compacts is due to the spin dependent intergranular tunneling influenced by the Coulomb gap.<sup>9,10</sup> A CrO<sub>2</sub>–I–Co tunneling junction using a native oxide barrier has also been reported with a small MR of about 1%,<sup>11</sup> and so far no large MR in single magnetic junction made with CrO<sub>2</sub> has been reported.

In this work we studied magnetic transport between nano-sized CrO<sub>2</sub> single domain particles. Cold-pressed CrO<sub>2</sub> nanopowders show a significant MR at low temperature. The transport mechanism has been understood as the intergranular tunneling. Using transmission electron microscopy (TEM), x-ray diffraction (XRD), and x-ray photoelectron spectroscopy (XPS), the tunneling barrier has been characterized to be a Cr<sub>2</sub>O<sub>3</sub> native oxide layer on the CrO<sub>2</sub> particle surface. In order to enhance the magnetotransport behavior of the tunneling effect between CrO<sub>2</sub> particles, needle-

shaped CrO<sub>2</sub> particles have been aligned using a strong magnetic field. The field-aligned particles show junction-like MR behavior with two well-separated peaks and the switching magnetic field is about 1000 Oe which is much lower than that of the cold-pressed powders.

## II. EXPERIMENTS AND DISCUSSIONS

### A. MR of cold-pressed CrO<sub>2</sub> nanopowders

Cold-pressed CrO<sub>2</sub> powder compacts were made with the nano-sized powders supplied by DuPont. The powders were analyzed by XRD and TEM. They are single crystal needle-shaped particles with lengths of about 400 nm and an aspect ratio of about 9:1. The coercivity is about 600 Oe at room temperature and about 1000 Oe at  $T=5$  K. Using a hardened-steel die, the cold-pressed compacts were made under a pressure of  $5 \times 10^8$  N/m<sup>2</sup>. The magnetization was measured with a superconducting quantum interference device magnetometer and the electron magnetotransport properties were measured with a Quantum Design physical properties measurement system (PPMS). The two-terminal method was used in the transport measurements and electrodes were made with silver print. The cold-pressed sample shows a resistivity of about 0.1  $\Omega$  cm at room temperature.

Figure 1 shows the negative MR of the cold-pressed CrO<sub>2</sub> sample at  $T=5$  K, where the MR is defined as  $(R_H - R_{H=0})/R_{H=0}$ . It reaches about 28% in a field of 5 T. The inset of Fig. 1 shows the MR over the low field range together with the magnetic hysteresis loop. One can see that the resistance reaches its maximum values coordinating to the reversing of the magnetic moments. The mechanism of this MR effect is understood to be a result of the electron spin dependent tunneling between neighboring CrO<sub>2</sub> particles.<sup>8–10</sup>

### B. MR of aligned CrO<sub>2</sub> nanopowders

From Fig. 1 one can see that the switching field (the magnetic field at which significant MR ratio has been

<sup>a)</sup> Author to whom correspondence should be addressed; electronic mail: jtang@uno.edu

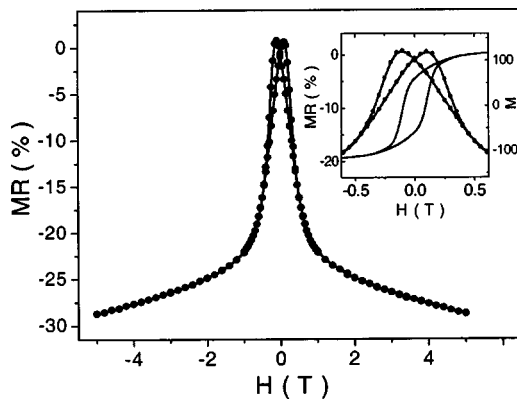


FIG. 1. MR of cold-pressed CrO<sub>2</sub> powder compact, measured at  $T=5$  K. Inset shows the low field MR together with the magnetization curve.

reached) of the cold-pressed powder is quite large. Normally the switching field for the powder compacts and polycrystalline films is larger than 1 T, which is too large for many applications. Basically, the value of the switching field corresponds to the external field at which the magnetic moments of particles (grains) are reversed. It is obvious that random orientation of moments may cause the overall switching field to become much larger than the coercivity of a single particle. This problem can be solved by finding a way to align the CrO<sub>2</sub> single crystalline particles to the same orientation. The switching field can be reduced theoretically to the coercivity field of a single particle.

In our experiment, since the magnetic moments of the needle-shaped CrO<sub>2</sub> single crystalline particles were along the easy axes ( $c$  axes), the particles can be reoriented by applying a strong magnetic field. The CrO<sub>2</sub> powders were added to ethanol with a 1:200 ratio, and an ultrasonic shaker was used to break the aggregates for uniform distribution of the CrO<sub>2</sub> particles in the suspension. The suspension was dropped onto a polymer substrate at room temperature in a magnetic field of 1 T. After drying, the needle-shaped CrO<sub>2</sub> particles became affixed to the substrate and were aligned along the direction of the magnetic field. Two electrode contacts were made by silver paste. The size of the measured samples was approximately 100  $\mu\text{m}$ , and the resistance was around 0.1 M $\Omega$  at room temperature, which was much larger than that of the cold-pressed powders. Figure 2 illustrates the aligned particles and the transport measurement.

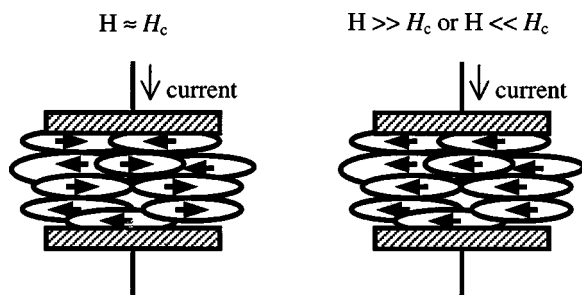


FIG. 2. Illustration of the field-aligned needle-shaped CrO<sub>2</sub> particles and the measurement of magnetotransport.

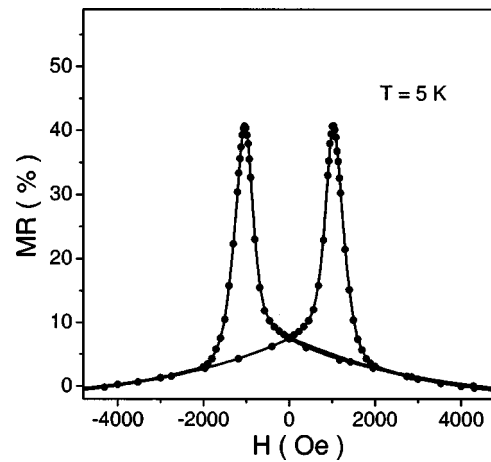


FIG. 3. MR of the field-aligned CrO<sub>2</sub> particles which shows a junction-like behavior with a low switching field of about  $\pm 1000$  Oe.

The aligned needle-shaped CrO<sub>2</sub> particles express a very interesting MR effect with two well-separated peaks, like a single magnetic tunneling junction, as shown in Fig. 3. Comparing to the cold-pressed powders in which the particles have random orientations, the junction-like MR of the aligned powders is about 41% at  $T=5$  K, and the switching field significantly decreases to about  $\pm 1000$  Oe. Notice that the resistance change is less than 5% for the random-orientated pressed powders over the same range of magnetic field. One can see that by using alignment technique, a much larger MR ratio can be reached over a low field range ( $0 \sim \pm 1000$  Oe), which shows a much better switching behavior than that of the random-oriented powder compacts.

Temperature dependence of the MR and resistivity  $R$  of the aligned CrO<sub>2</sub> particles were measured and results are shown in Fig. 4 and its inset, respectively. One sees that the  $\ln R$  is proportional to  $1/T^{1/2}$  at low temperature ( $< 50$  K), which is typical in the intergranular tunneling. It is known that the temperature dependence of intergranular tunneling resistance follows<sup>12-14</sup>

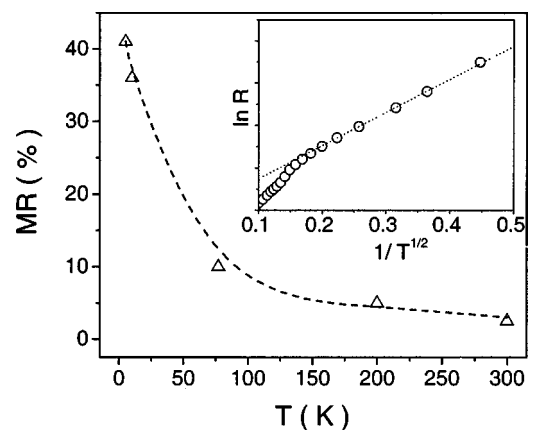


FIG. 4. Temperature dependence of the MR of the aligned CrO<sub>2</sub> powders. The inset shows the logarithmic resistance  $\ln R$  as a function of  $T^{1/2}$ , the resistance is 99.4 k $\Omega$  at 300 K and increases to 893 k $\Omega$  at 5 K.

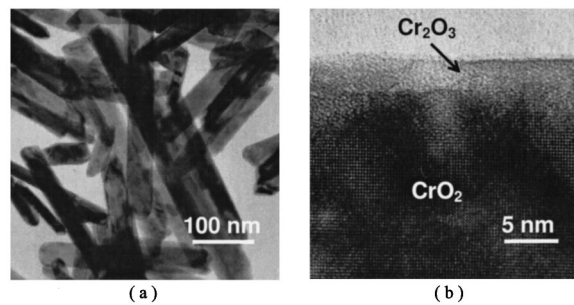


FIG. 5. (a) TEM micrographs of the needle-shaped  $\text{CrO}_2$  nanoparticles. (b) A high-resolution image clearly shows a thin layer on the surface of the single crystal  $\text{CrO}_2$ .

$$R \sim \exp(\Delta/T)^{1/2}, \quad (1)$$

where  $\Delta$  is proportional to the Coulomb charging energy and barrier thickness. The Fig. 4 inset shows that the  $\ln R$  is linear to  $1/T^{1/2}$  and indicates that the intergranular tunneling is the major conducting mechanism at low temperature. With increasing temperature, the resistance decreases faster than Eq. (1), which implies that some other conducting channels become larger. MR also decreases quickly with increasing temperature as Fig. 4 shows. This phenomenon can be correlated to the spin-flip effects, which becomes significant at high temperature, and suppresses the spin dependent conduction. Several spin-flip mechanisms have been introduced.<sup>9,15,16</sup> It is found in our work that the spin dependent tunneling MR between  $\text{CrO}_2$  particles can be relatively suppressed by an spin independent conducting channel, which is due to the high-order inelastic hopping. The details about inelastic hopping is discussed in another article.<sup>17</sup>

### C. Microstructure of the intergranular tunneling barrier

For the intergranular tunneling systems of  $\text{CrO}_2$  powder compacts or polycrystalline films, the role of the tunneling barrier was suggested to be played by the grain boundary,<sup>8,9</sup> and the barrier material was expected to be composed of  $\text{Cr}_2\text{O}_3$  since it is the most stable phase of chromium oxides.<sup>2,11,18</sup> In our experiments performed using TEM, XRD, and XPS, etc., hard evidence of the existence of the  $\text{Cr}_2\text{O}_3$  boundary layer were found, and intergranular tunneling barrier was well-characterized.

Using TEM, we directly observed a 1–3 nm thick native oxide layer on the surface of the  $\text{CrO}_2$  single crystal particles. Figure 5(a) shows the TEM image of the  $\text{CrO}_2$  single crystal particles which has a needle shape and a diameter of about 50 nm. Figure 5(b) is the high-resolution lattice image of the  $\text{CrO}_2$  particle with an [001] axis along its length, showing clearly the thin layer on the surface of the single crystal  $\text{CrO}_2$ . This layer was observed on every particle.

XPS measurement was performed, and the results suggested that the  $\text{Cr}^{3+}$  dominated in the near surface region ( $\sim 10$  monolayers) of the  $\text{CrO}_2$  particles. One should notice that XPS is sensitive within 10–20 Å into the particle surface. Our result indicated that the 1–3 nm thick surface layer

on the  $\text{CrO}_2$  particles was not  $\text{CrO}_2$  but a  $\text{Cr}^{3+}$  compound. The result confirmed the expectation that a  $\text{Cr}_2\text{O}_3$  native oxide layer existed on the  $\text{CrO}_2$  surface,<sup>8–11</sup> and this insulator layer played the role of the tunneling barrier. This result was also supported by a very slow scan of XRD experiment, which showed that a small amount (5%–10%) of crystalline  $\text{Cr}_2\text{O}_3$  existed in the “pure”  $\text{CrO}_2$  powders.

### III. SUMMARY AND CONCLUSIONS

We have studied the magnetic properties and magnetotransport of cold-pressed  $\text{CrO}_2$  nanopowders; the large MR ratio corresponded to the spin dependent intergranular tunneling effect. By using field-introduced order, the needle-shaped  $\text{CrO}_2$  nanoparticles were aligned along the same direction and exhibited texture structure. The magnetotransport of the aligned  $\text{CrO}_2$  nanoparticles showed a junction-like MR behavior with a low switching field of about 1000 Oe. It also showed a large MR ratio of about 41% at  $T=5$  K. The MR ratio decreased with the increasing of temperature, which was due to the spin independent conduction becoming dominant at high temperature. The microstructure of the intergranular tunneling system was analyzed using TEM together with XPS and XRD. A very thin layer of  $\text{Cr}_2\text{O}_3$  was observed and characterized on the surface of the  $\text{CrO}_2$  particles, which confirmed that the role of the intergranular tunneling barrier was played by  $\text{Cr}_2\text{O}_3$ .

The authors thank Dr. H. Xu, L. Spinu, F. Chen, W. Wang, M. Li, and U. Deblod for their assistance in measurements and discussions. This work was supported by the Louisiana Board of Regent Support Fund Grant No. LEQSF (2000-03)-RD-B-10 and Sharp Laboratories of America.

<sup>1</sup>K. Schwarz, J. Phys. F: Met. Phys. **16**, L211 (1986).

<sup>2</sup>K. P. Kamper, W. Schmitt, and G. Guntherodt, Phys. Rev. Lett. **59**, 2788 (1987).

<sup>3</sup>R. J. Soulen, J. M. Byers, M. S. Osofsky, B. Nadgorny, T. Ambrose, S. F. Cheng, P. R. Broussard, C. T. Tanaka, J. Nowak, J. S. Moodera, A. Barry, and J. M. D. Coey, Science **282**, 85 (1998).

<sup>4</sup>R. Wiesendanper, H. J. Guntherodt, G. Guntherodt, R. J. Gambino, and R. Ruf, Phys. Rev. Lett. **65**, 247 (1990).

<sup>5</sup>J. S. Moodera, L. R. Kinder, T. M. Wong, and R. Meservey, Phys. Rev. Lett. **74**, 3273 (1995).

<sup>6</sup>H. Y. Hwang and S. W. Cheong, Science **278**, 1607 (1997).

<sup>7</sup>K. Suzuki and P. M. Tedrow, Appl. Phys. Lett. **74**, 428 (1999); Phys. Rev. B **58**, 11597 (1998).

<sup>8</sup>S. S. Manoharan, D. Elefant, G. Reiss, and J. B. Goodenough, Appl. Phys. Lett. **72**, 984 (1998).

<sup>9</sup>J. M. D. Coey, A. E. Berkowitz, L. Balcells, and F. F. Putris, Phys. Rev. Lett. **80**, 3815 (1998).

<sup>10</sup>M. Garcia-Hernandez, F. Guinea, A. Andres, J. L. Martinez, C. Prieto, and L. Vazquez, Phys. Rev. B **61**, 9549 (2000).

<sup>11</sup>A. Barry, J. M. D. Coey, and M. Viret, J. Phys.: Condens. Matter **12**, L173 (2000).

<sup>12</sup>J. Inoue and S. Maekawa, Phys. Rev. B **53**, 11929 (1996).

<sup>13</sup>S. Mitani, S. Takahashi, K. Takanashi, K. Yakushiji, S. Maekawa, and H. Fujimori, Phys. Rev. Lett. **81**, 2799 (1998).

<sup>14</sup>T. Zhu and J. Wang, Phys. Rev. B **60**, 11918 (1999).

<sup>15</sup>C. H. Shang, J. Nowak, R. Jansen, and J. S. Moodera, Phys. Rev. B **58**, 2917 (1998).

<sup>16</sup>S. M. Watts, S. Wirth, S. V. Molnar, A. Barry, and J. M. D. Coey, Phys. Rev. B **61**, 9621 (2000).

<sup>17</sup>J. Dai and J. Tang, Phys. Rev. B **63**, 64410 (2000).

<sup>18</sup>P. S. Robbert, H. Geisler, C. A. Ventrice, J. van Ek, S. Chaturvedi, J. A. Rodriguez, M. Kuhn, and U. Diebold, J. Vac. Sci. Technol. A **16**, 990 (1998).